Optics & Laser Technology 45 (2013) 336–341

Contents lists available at SciVerse ScienceDirect

Optics & Laser Technology

journal homepage: www.elsevier.com/locate/optlastec

Detection of stain formation on teeth by oral antiseptic solution using fiber optic displacement sensor

H.A. Rahman [a,b,d], H.R.A. Rahim [e,f], S.W. Harun [a,b,*], M. Yasin [b,c], R. Apsari [c], H. Ahmad [b], W.A.B Wan Abas [e]

[a] Department of Electrical Engineering, Faculty of Engineering, University of Malaya, 50603 Kuala Lumpur, Malaysia
[b] Photonics Research Centre, Department of Physics, Faculty of Science, University of Malaya, 50603 Kuala Lumpur, Malaysia
[c] Department of Physics, Faculty of Science and Technology, Airlangga University, Surabaya 60115, Indonesia
[d] Faculty of Electrical Engineering, Universiti Teknologi MARA (UiTM), 40450 Shah Alam, Malaysia
[e] Department of Biomedical Engineering, Faculty of Engineering, University of Malaya, 50603 Kuala Lumpur, Malaysia
[f] Faculty of Electronic & Computer Engineering, Universiti Teknikal Malaysia Melaka (UTeM), Hang Tuah Jaya, 76100 Durian Tunggal, Melaka, Malaysia

ARTICLE INFO

Article history:
Received 31 March 2012
Received in revised form
6 June 2012
Accepted 20 June 2012
Available online 12 July 2012

Keywords:
Fiber optic displacement sensor
Oral antiseptic solution concentration
Dental color matching system

ABSTRACT

The application of a simple intensity modulated fiber optic displacement sensor for the detection of stain formation on human teeth is demonstrated. The proposed sensor uses a concentric type bundled plastic optical fiber (POF) as a probe in conjunction with the surfaces of five human teeth as the reflecting targets. Prior to the experiment, the stains were produced extrinsically by soaking the teeth in different concentrations of oral antiseptic solution containing hexetidine. The concentration of the oral antiseptic solution is measured in volume%. For a concentration change from 0% to 80%, the peak voltage decreases exponentially from 1.15 mV to 0.41 mV with a measured resolution of 0.48% and 1.75% for concentration ranges of 0–40% and 40–80%, respectively. The correlation between the detector output and variation in the color of human tooth surface has successfully been examined. Simple in design and low in cost, this sensor can detect color changes due to hexetidine-induced stain on a tooth surface in a fast and convenient way. Thus, this sensor will be very promising in esthetic dentistry, dental color matching techniques, chemical and biomedical applications.

1. Introduction

In the last few decades, dental clinicians face increasing demands and expectations for accurate color matching due to the increasing attention given by the media and patients to esthetic dentistry. Hence, precise color matching has become an even more critical success factor for esthetic restoration. The subjective color perception of an observer leads to variations and unpredictable differences in color evaluation and matching among clinicians. Among the elements that affect the perceived color are the spectral distribution of a color stimulus, the surroundings of the stimulus [1], the state of an observer's visual system and on the observer's experience [2]. Furthermore, different surroundings lead to metamerism which is a phenomenon whereby different colors are exhibited by the same tooth when viewed under different lighting conditions [3].

Conventionally, clinicians used visual shade guides for tooth color matching. The use of shade guides is a quick and cost-effective method but its success depends strongly on professional experience [4]. Recently, significant advances have occurred in techniques and instruments for colorimetric analysis in dentistry which minimizes the subjective variance in the color matching process. These devices can be categorized as spectrophotometers, colorimeters, digital color analyzers or combinations of these. These devices have been demonstrated to be useful in quantifying color differences [5–9]. A spectrophotometer measures the spectral reflectance or transmittance curve of a specimen. In comparison to colorimeters, they have a longer working life but are more complex and expensive [5]. Colorimeters measure color tristimulus values from light reflected from the specimen. A series of photodiode filters are used to control light reaching the specimen. The repeatability of colorimeters may deteriorate with the aging of the filters [10]. Digital color analyzers have gained much popularity but the quality of the images are also influenced by lighting conditions and as such the integrity of the results are questionable [11].

Fiber optic displacement sensors (FODS) may potentially evolve into a new choice of dental color matching system featuring more advantages and potential. They are commonly constructed from multimode plastic optical fibers (POFs), which offer the benefit of low optical signal transmission loss, low

* Corresponding author at: Department of Electrical Engineering, University of Malaya, 50603 Kuala Lumpur, Malaysia.
E-mail address: swharun@um.edu.my (S.W. Harun).

0030-3992/$ - see front matter © 2012 Elsevier Ltd. All rights reserved.
http://dx.doi.org/10.1016/j.optlastec.2012.06.027

production cost, compact size and compatibility with optical fiber technology. Three distinct methods are competent and commonly used for the displacement measurement: laser interferometry, wavelength modulation and the reflective intensity modulation technique. Laser interferometry [12] is based on fringe counting and offers high resolution and stability of measurement. However, its precision and stability are dependent on the wavelength of light. Wavelength modulation need fiber Bragg grating (FBG) and optical spectrum analyzer (OSA) for physical parameter detection and data acquisition, respectively, which are very costly. The intensity modulated-based sensors use the modulation of light power transmitted between the head of the sensor and the target surface [13]. In comparison with the first two methods for displacement measurements, the light intensity modulation is the simplest method to obtain a high resolution measurement. The intensity modulated sensors compete well with other sensing methods as they are relatively inexpensive, contactless, easy to be fabricated and suitable for employment in harsh environments. These type of sensors have been demonstrated to be efficient for measuring various types of surface profiles [14–16].

Most light intensity modulated displacement sensors operate by utilizing two parallel adjacent fibers (one for transmitting and the other for receiving light) [14–17] as they provide good sensing outcome. Polygerinos et al. [18] demonstrated the improved performance of an intensity modulated FODS by the use of a single optical fiber. Another research by Yasin et al. demonstrated the applicability of using concentric bundled fibers POFs with various number of receiving fibers and discovered that the sensitivity of a displacement sensor increases with the increasing number of receiving fibers within the bundled fiber [19]. This is mainly due to the increased total surface area on account of the increasing number of receiving fibers. He later attempted to compare the performances of a concentric bundled POF (consisting of one transmitting fiber and 16 receiving fibers) and a single transmitting and receiving fiber (multimode fused coupler) [20]. In terms of sensitivity, the former outperformed the latter by more than double its value but is inferior in terms of the operating displacement range. The use of concentric bundled POFs are especially advantageous in dental applications as they have rougher surface and tend to reflect light at various directions.

In the work presented here, we propose and demonstrate a simple intensity modulated fiber optic displacement sensor using a concentric bundled POF as well as teeth surfaces as reflecting targets. POFs are used as they offer the same advantages as conventional silica optical fibers but involve simpler and less expensive components. Furthermore, they possess greater flexibility and fracture toughness and the relatively large diameter (1 mm) of the multimode POF eases the handling and alignment process. In our approach, variations of colors are achieved via immersion of the teeth in different oral antiseptic solution concentration in de-ionized water as they are known for their negative effect in teeth staining [21–24]. This technique offers simplicity, reliability and continuous measurement capability. In addition, it is suitable for measuring color changes of teeth undergoing bleaching treatments.

2. Experimental setup

Fig. 1 shows the schematic diagram of the fiber optic displacement sensor which is employed for the detection of teeth stains. The sensor consists of a fiber optic transmitter, mechanical chopper, fiber optic probe, five flat human teeth surfaces, a silicon photo detector, lock-in amplifier and a computer. The fiber optic probe is made of two 2 m long polymethyl methacrylate (PMMA) which consists of one transmitting core of 1 mm in diameter and 16 receiving cores of 0.25 mm in diameter, numerical aperture of 0.5, core refractive index of 1.492 and cladding refractive index of 1.402. The output signal (reflected signal) is the power sum of each of the receiving fibers [25]. A red He–Ne laser ($\lambda = 633$ nm) was used as the light source with an average output power of 5.5 mW, beam diameter of 0.80 mm and beam divergence of 1.01 mrads. The photodetector is a high speed silicon photodiode with an optical response of 400–1100 nm, making it compatible with a wide range of visible light including the 633 nm visible red He–Ne laser used in this setup. The light source was modulated externally by a chopper with a frequency of 113 Hz as to avoid the harmonics from the line frequency which is about 50–60 Hz. The modulated light source was used in conjunction with a lock-in amplifier to reduce the dc drift and interference of ambient stray light.

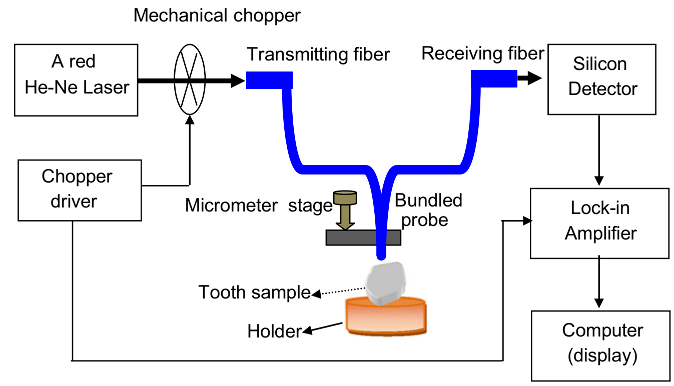

Fig. 1. Schematic diagram of the fiber optic displacement sensor for the detection of stain on human teeth.

The displacement of the fiber optic probe was achieved by mounting it on a micrometer translation stage, which was rigidly attached to a vibration free table. Light from the fiber optic transmitter (peak wavelength at 633 nm) was coupled into the transmitting core. The signal from the receiving cores was measured by moving the probe away from the zero point, where the reflective surface of the teeth samples and the probe were in close contact. The signal from the detector was converted to voltage and measured by a lock-in amplifier and computer via RS232 using a Delphi software.

Five human teeth, namely canine teeth were extracted and stored in water at room temperature one week prior to the experiments. The teeth surfaces were cut to produce smooth and flattened surfaces of equal height. The probe can be adjusted to obtain the maximum reflected light as to ensure that the probe and the tooth surface are perpendicular to each other. One of the teeth samples was used as the control sample while the other four were soaked for a duration of 24 h in oral antiseptic solutions (Bactidol, 0.1% hexetidine, Interphil Laboratories Inc., Singapore) with concentrations of 20, 40, 60 and 80 ml diluted with de-ionized water to a total volume of 100 ml. Each of the five teeth samples was used consecutively as the reflecting target whilst measuring the output intensity by changing the position of the fiber optic probe from 0 to 2.5 mm in a step of 50 µm. There was no actual contact between the probe and the tooth surface as the zero displacement actually refers to a very small distance between them. In preparation for the experiment, the teeth were removed from the antiseptic solution and left dried without being washed. During the experiment, the temperature was kept constant at 25 °C and the error due to this temperature variation is negligible. The use of the same type of teeth surfaces and teeth dimension reduces the error due to variation in teeth surface roughness.

3. Results and discussions

Fig. 2 shows the reflected light intensity versus displacement of the fiber optic probe from teeth surfaces with varying amounts of stain intensity. All curves exhibit a maximum with a gradual and linear increase in the front slope while the back slope follows an almost inverse square law relationship. When the displacement is increased, more light will be collected by the receiving cores due to the increased size of the reflected cone of light. A further increase in the displacement leads to larger overlapping which results in a further increase in the output power as seen in the first part of the curve until a certain peak value is achieved. At this peak value, the reflected cone power falls within the surface area of the receiving fiber. Further increase of the displacement will result in a reflected cone size bigger than the size of the receiving fibers. Therefore, only a fraction of the power of the reflected light will be detected, as seen in the second part of the curve. The decrement of the received light intensity with increasing concentration is due to the change of the refractive index at the teeth surfaces, which actually changes the angle of the reflected light beam. In ideal cases (when the reflecting target is flat and smooth, i.e. a flat mirror), the starting points of the curves would be near zero and coincidental. Since teeth in general have a higher surface roughness and are more uneven than that of a mirror, the observed curves start at a much higher point and do not coincide among each other. However, this does not affect the performance of the sensor since the evaluation is based on the peak voltage and the second slope of the displacement profiles which are independent of the inconsistencies mentioned earlier.

The reflection of light from a surface is based on the concept of geometrical optics and can be explained using Fig. 3 [25]. Several assumptions need to be made in order to analyze the displacement sensing characteristics theoretically. Firstly, the bundled fiber in front of the mirror is modeled as a set of three independent parallel fibers, which is assumed to be in contact with each other with no space left between them. Secondly, both of the transmitting and receiving fibers are assumed to have perfectly circular cross sections with areas of S_a and S_b and radii of w_a and w_b, respectively, as shown in Fig. 3. The light leaving the transmitting fiber is represented by a perfectly symmetrical cone with a half-divergence angle of a, and the vertex O is located at a distance of z_a inside the fiber end of plane 1. In the analysis, the light cone from the transmitting fiber (plane 1) is extended beyond the mirror plane (plane 2), and the image position at the receiving end (plane 3) is analyzed to determine the amount

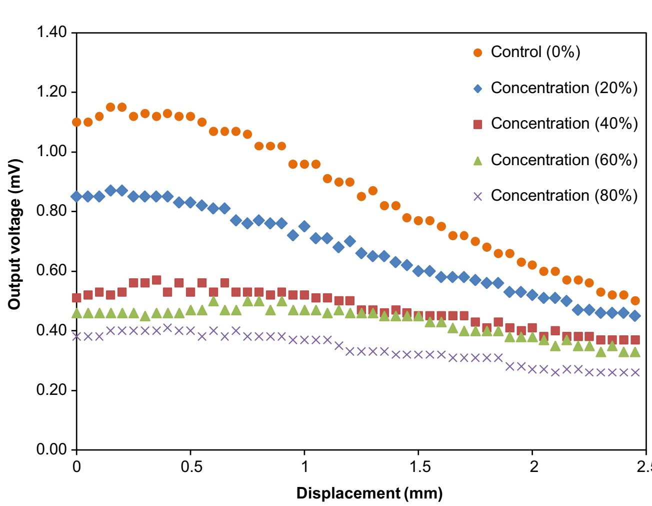

Fig. 2. Variation of output voltage against displacement.

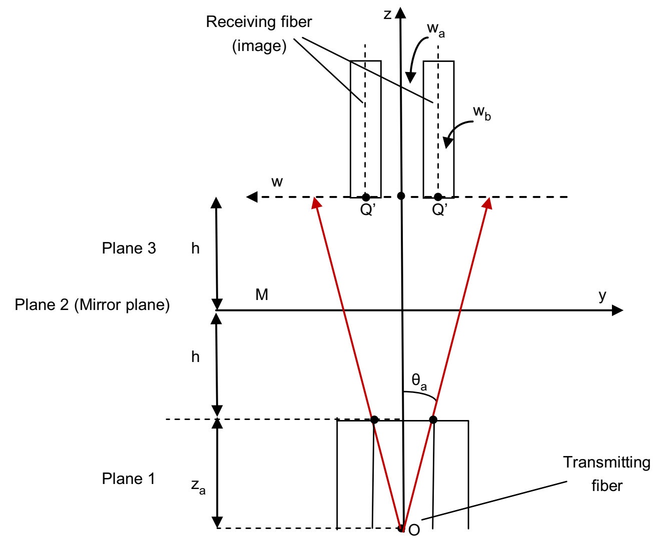

Fig. 3. Cone of light exiting the transmitting fiber.

of light received by the receiving fibers. The z-axis represents the direction of the emitted light cone centered at O and extending beyond the mirror surface. The coordinates of the center point in the receiving fiber's cores end are Q_0 and are represented by

$$Q' \begin{cases} y = \frac{5}{4} w_a \\ z = z_a + 2h \end{cases} \tag{1}$$

where $w_a = 4w_b$ and h is the distance being monitored.

An electromagnetic Gaussian beam approach is used to theoretically determine the transfer function of the sensor. This approach describes the light leaving the transmitting fiber bundle as a paraxial beam with a Gaussian profile. The irradiance of the emitted light decreases exponentially over the radial beam cross-sections, according to

$$I(r,z) = \frac{2P_E}{\pi w^2(z)} \exp\left(-\frac{2r^2}{w^2(z)}\right) \tag{2}$$

where r is the radial coordinate, z is the longitudinal coordinate, and the radius $w(z) = w_o\sqrt{1+(z/z_R)^2}$ is a measure of the beam width whose dependence is on z. P_E is the emitted power at point O. The constants w_o and z_R are the waist radius and Rayleigh length, respectively, and their relationship is given by

$$\pi {w_o}^2 = \lambda z_R. \tag{3}$$

The beam resembles a spherical wave confined within a cone for points situated in the far-field zone ($z \gg z_R$) as depicted in Fig. 3. The cone is characterized by a divergence angle given by (small angle approximation)

$$\theta_a \approx \tan\theta_a = \frac{w(z)}{z} = \frac{w_o}{z_R} = \frac{\lambda}{\pi w_o} \tag{4}$$

and the irradiance function can be simplified as

$$I(r,z) = \frac{2P_E}{z^2 \pi {\theta_a}^2} \exp\left(-\frac{2r^2}{{\theta_a}^2 z^2}\right). \tag{5}$$

By integrating $I(r,z)$ over the fiber end surface S_b, we obtain the optical power collected by the receiving fiber

$$P(z) = \int_{S_b} I(r,z)dS. \tag{6}$$

By assuming that the irradiance $I(r,z)$ is approximately constant across the receiving surface with an area $S_a = \pi w_a^2$,

$S_b = \pi w_b^2 = 1/16\pi w_a^2$ and equal to its value at the center of the receiving fiber (point Q') where $r = 5/4w_a \approx \theta_a z_a$, we obtain

$$P = IS_b = \frac{2P_E}{\zeta^2}\exp\left(-\frac{25}{8\zeta^2}\right), \tag{7}$$

where

$$\zeta = \frac{z}{z_a} = 1 + \frac{2h}{z_a} = 1 + 2h_N \tag{8}$$

and h_N is the normalized distance. By evaluating $dP/d\zeta = 0$, the maximum collected power is obtained as $P_{max} = 16P_E/(25e)$. Eq. (7) can be written in normalized form, $P_N = P/P_{max}$ as

$$P_N = \frac{25}{8\zeta^2}\exp\left(1 - \frac{25}{8\zeta^2}\right) \tag{9}$$

Taking into account that the transfer function was derived for a flat mirror as the reflector with 100% reflectivity, the normalized power when tooth surface is used as the reflector would be

$$P_{Nnew} = RP_N \tag{10}$$

where R is the reflectivity of the tooth surface.

The reflectivity of canine tooth surface was obtained at 4.18% by comparing the power of the light source before and after the reflecting surface. Hence, the transfer function becomes

$$P_N = \frac{1.045}{8\zeta^2}\exp\left(1 - \frac{25}{8\zeta^2}\right) \tag{11}$$

The relationship between the peak voltages and the antiseptic concentrations is depicted in Fig. 4(a), and subsequently Fig. 4(b) shows the curve of the second slope of the displacement profiles against the antiseptic concentrations. Both of the peak voltages and the second slope of displacement profiles decrease exponentially with the concentration but the former has a steeper slope and better fit than the latter. The adjusted r^2 value or the coefficient of determination is the measure of the goodness of fit. The adjusted r^2 value of the output based on the peak voltage and the second slope of the displacement profiles are 0.9761 and 0.9694, respectively. The considerably high values of the adjusted r^2 allow the prediction of unknown concentrations by the model.

The linearity analyses based on the peak voltages and second slope of displacement profiles at variance with 0–40% concentrations and 40–80% concentrations are depicted in Fig. 5(a) and (b), respectively. In both the graphs, the peak voltage based analysis produces a better sensitivity than the second slope based analysis. Furthermore, it is observed that the 0–40% concentration range is more sensitive than the 40–80% concentration range with an increased sensitivity of more than 3 times for the peak voltage based analysis and more than 6 times for the second slope based analysis.

Table 1 summarizes the performance of the FODS for human teeth samples based on the analysis of the peak voltage. It is observed that the sensor is sufficiently stable with a maximum standard deviation of 0.78% with a linearity of more than 99% for both of the concentration ranges of 0–40% and 40–80%. The first range exhibit better performance with a sensitivity and resolution of 0.0145 mV/% and 0.48%, respectively, compared to those of the second range which are 0.004 mV/% and 1.76%, respectively. The resolution is obtained by calculating the ratio of the maximum standard deviation (0.007 mV) to the sensor's sensitivity (mV/%).

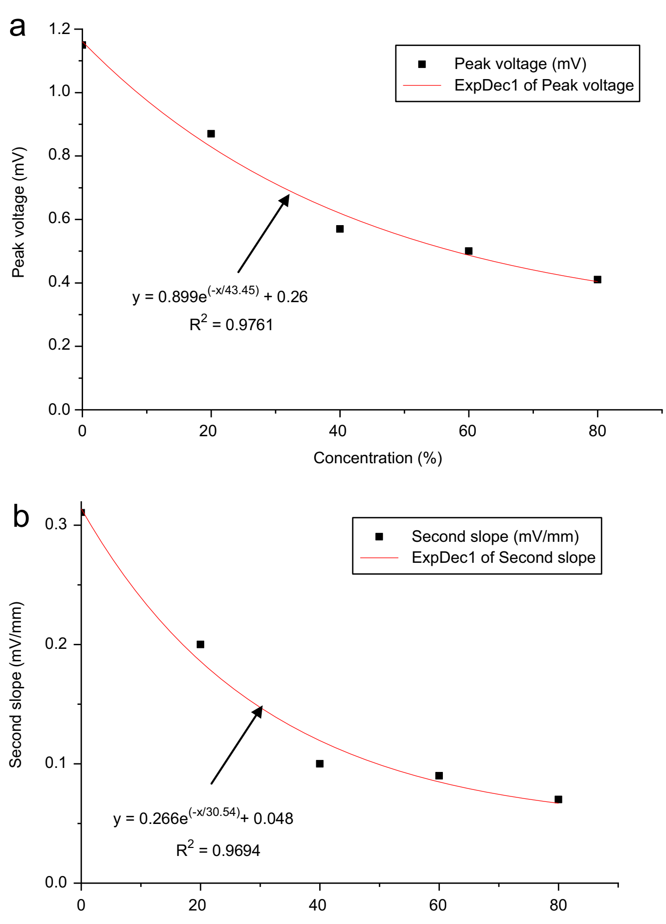

Fig. 4. (a) Peak voltage and (b) second slope of displacement profile versus concentration of various oral antiseptic solution concentrations.

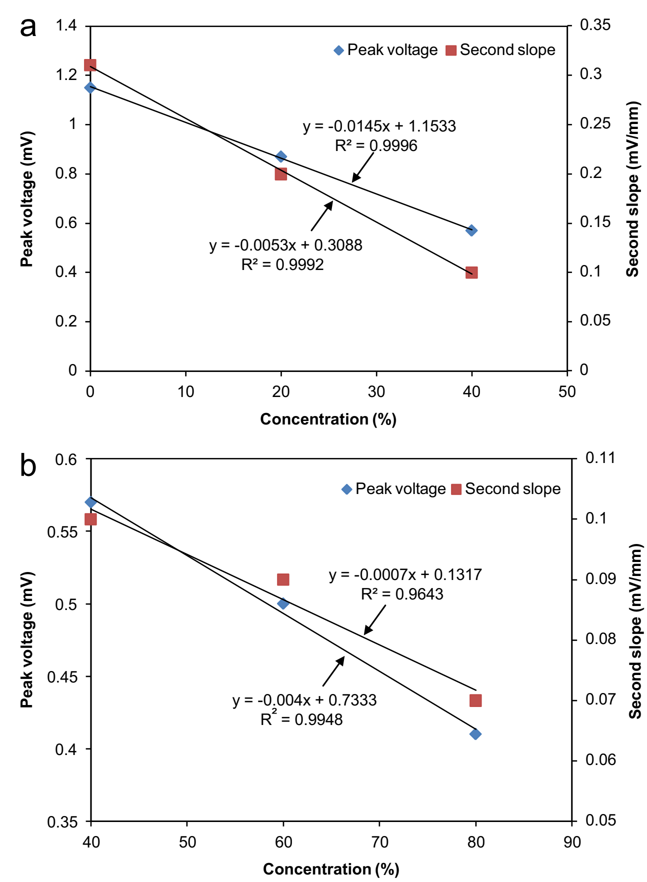

Fig. 5. Peak voltage (left column) and second slope of displacement profile (right column) versus (a) 0–40% concentration and (b) 40–80% concentration of various oral antiseptic solution concentrations.

Table 1
The performance of FODS for the detection of stained human teeth.

Parameter	0–40%	40–80%
Sensitivity (mV/%)	0.0145	0.004
Linear range (%)	0–40	40–80
Linearity (%)	99	99
Standard deviation	0.0026–0.007 mV (0.46–0.78%)	0.0026–0.007 mV (0.46–0.78%)
Resolution (%)	0.48	1.75

The diluted oral antiseptic solution containing 0.1% of hexetidine used in the experiment induces significantly less staining compared to other antiseptics [26]. Hence the resolution is considerably good since 0.48% and 1.76% of the oral antiseptic concentration represent only a small change in stain intensity variation which is barely seen by the naked eye. Possible sources of error in the sensor operation are likely due to light source fluctuation, stray light and possible mechanical vibrations. To reduce these effects a well-regulated power supply is used for the red He–Ne laser and this minimizes the fluctuation of source intensity. The sensor fixture is also designed so that the stray light cannot interfere with the source light and room light does not have any effect on the output voltage. To reduce the mechanical vibrations, the experimental setup is arranged on a vibration free table. For practical use, a cheaper alternative would be to use optical breadboards which can be integrated with a larger system that include vibration control systems.

These preliminary results indicate the capability of implementation of the FODS for the detection of stain formation on teeth by oral antiseptic solution containing 0.1% hexetidine. The use of a micrometer translation stage for displacements and known concentrations of the antiseptic solution provide calibration for the displacement and concentration (0–80%), respectively. Based on the results, unknown concentrations can be determined from the experimentally derived exponential equation (Fig. 3). Future work involve the extension of the scope to a wider range of source frequency spectrum, the use of different types of teeth surfaces and the consideration of various other causes of tooth discoloration (direct and indirect stains). Furthermore, extension to in vivo based research need to be implemented with the inclusion of additional sensors into the probe for automatic angle measurements and control. In order to function as a reliable dental color matching instrument, the accuracy and precision of the device must be evaluated in a clinical setting.

Among the other color matching techniques in dentistry, spectrophotometers are the most accurate and flexible. It was reported that spectrophotometers offered a 33% increase in accuracy and a more objective match in 93.3% cases compared to conventional techniques [10,27]. In spite of the superior accuracy and reliability, the majority of dental practitioners sort to the traditional way of using visual shade guides and colorimeters due to the high cost and complexity involved. With the use of a commercially available POF, source and detector for the proposed technique, the setup proves to be simple, sensitive, low cost and light in weight hence has potential to compete as a choice of dental color matching technique.

4. Conclusions

Detection of stain formation on human teeth by oral antiseptic solution is demonstrated by using fiber optic FODS. The effect of oral antiseptic solution concentrations on the displacement curve is investigated. As the concentration of oral antiseptic solution increases, both the received light intensity and second slope of the displacement profile decrease. This is attributed to the reduction of the received light intensity occasioned by the change of the refractive index at the teeth surface, which in turn changes the angle of the reflected light beam. Additionally, the sensor has better performance within the 0–40% concentration range as compared to the 40–80% concentration range. This proposed setup provides numerous advantages such as simplicity of design, low cost of production, contactless and non-destructive.

Acknowledgment

The authors are grateful to Dr. Suhaila Abdullah and Dr. Mohd Noor Fareezul Noor Shahidan for providing the human teeth samples used in this experiment. This work is financially supported by University of Malaya under PPP grant scheme (no: PV033/2011A) and HIR-MOHE (no: D0000009-16001).

References

[1] Lee Y, Yu B, Lim JI, Lim H. Perceived color shift of a shade guide according to the change of illuminant. Journal of Prosthetic Dentistry 2011;105(2):91–9.
[2] Jaju RA, Nagai S, Karimbux N, Da Silva JD. Evaluating tooth color matching ability of dental students. Journal of Dental Education 2010;74(9):1002–10.
[3] Watts A, Addy M. Tooth discolouration and staining: a review of the literature. British Dental Journal 2001;190(6):309–16.
[4] Capa N, Malkondu O, Kazazoglu E, Calikkocaoglu S. Evaluating factors that affect the shade-matching ability of dentists, dental staff members and laypeople. Journal of the American Dental Association 2010;141(1):71–6.
[5] Tung FF, Goldstein GR, Jang S, Hittelman E. The repeatability of an intraoral dental colorimeter. Journal of Prosthetic Dentistry 2002;88(6):585–90.
[6] Jarad FD, Russell MD, Moss BW. The use of digital imaging for color matching and communication in restorative dentistry. British Dental Journal 2005;199(1):43–9.
[7] Da Silva JD, Park SE, Weber H, Dent M, Ishikawa-Nagai S. Clinical performance of a newly developed spectrophotometric system on tooth color reproduction. Journal of Prosthetic Dentistry 2008;99(5):361–8.
[8] Tung O, Lai Y, Ho Y, Chou I, Lee S. Development of digital shade guides for color assessment using a digital camera with ring flashes. Clinical Oral Investigations 2011;15(1):49–56.
[9] Odaira C, Itoh S, Ishibashi K. Clinical evaluation of a dental color analysis system: the Crystaleye Spectrophotometer®. Journal of Prosthodontic Research 2011;55(4):199–205.
[10] Chu SJ, Trushkowsky RD, Paravina RD. Dental color matching instruments and systems. Review of clinical and research aspects. Journal of Dentistry 2010;38:e2–16.
[11] Wee AG, Lindsey DT, Kuo S, Johnston WM. Color accuracy of commercial digital cameras for use in dentistry. Dental Materials 2006;22(6):553–9.
[12] Shirinzadeh B, Teoh PL, Tian Y, Dalvand MM, Zhong Y, Liaw HC. Laser interferometry-based guidance methodology for high precision positioning of mechanisms and robots. Robotics and Computer-Integrated Manufacturing 2010;26:74–82.
[13] Yasin M, Harun SW, Kusminarto Karyono, Ahmad H. Fiber-optic displacement sensor using a multimode bundle fiber. Microwave and Optical Technology Letters 2008;50(3):661–3.
[14] Golnabi H. Surface profiling using a double-fiber optical design. Optics and Lasers in Engineering 2010;48(4):421–6.
[15] Golnabi H. Design and operation of a double-fiber scanning system for surface profiling. Optics and Lasers in Engineering 2011;49(8):1032–9.
[16] Khorramnazari K, Golnabi H. Object surface characteristics monitoring using light reflection measurements. Journal of Applied Sciences 2011;11(15):2823–9.
[17] Binu S, Kochunarayanan K, Mahadevan Pillai VP, Chandrasekaran N. PMMA (polymethyl methacrylate) fiber optic probe as a noncontact liquid level sensor. Microwave and Optical Technology Letters 2010;52(9):2114–8.
[18] Polygerinos P, Seneviratne LD, Althoefer K. Modeling of light intensity-modulated fiber-optic displacement sensors. IEEE Transactions on Instrumentation and Measurement 2011;60(4):1408–15.
[19] Yasin M, Harun SW, Abdul-Rashid HA, Kusminarto, Karyono, Ahmad H. The performance of a fiber optic displacement sensor for different types of probes and targets. Laser Physics 2008;5(1):55–8.
[20] Yasin M, Harun SW, Pujiyanto ZA, Ghani, Ahmad H. Performance comparison between plastic-based fiber bundle and multimode fused coupler as probes in displacement sensors. Laser Physics 2010;20(10):1890–3.
[21] Addy M, Mahdaviand SA, Loyn T. Dietary staining in vitro by mouthrinses as a comparative measure of antiseptic activity and predictor of staining in vivo. Journal of Dentistry 1995;23(2):95–9.
[22] Ernst CP, Canbek K, Dillenburger A, Willershausen B. Clinical study on the effectiveness and side effects of hexetidine and chlorhexidine mouthrinses

versus a negative control. Quintessence International (Berlin, Germany) 2005;36(8):641–52.
[23] Sulieman M. An overview of tooth discoloration: extrinsic, intrinsic, and internalized stains. Dental Update 2005;32(8):463–71.
[24] Sulieman MA. An overview of tooth-bleaching techniques: chemistry, safety and efficacy. Periodontology 2000 2008;48(1):148–69.
[25] Yasin M, Harun SW, Karyono Kusminarto, Zaidan AH, Thambiratnam K, Ahmad H. Design and operation of a concentric-fiber displacement sensor. Fiber and Integrated Optics 2009;28(4):301–9.
[26] Addy M, Moran J. The formation of stain on acrylic surfaces by the interaction of cationic antiseptic mouthwashes and tea. Journal of Biomedical Materials Research 1984;18(6):631–41.
[27] Paul S, Peter A, Pietrobon N, Hammerle CH. Visual and spectral photometric shade analysis of human teeth. Journal of Dental Research 2002;81(8): 578–82.